Chance-constrained stochastic MPC of Astlingen urban drainage benchmark network

Control Engineering Practice

Svensen, Jan Lorenz; Sun, Congcong; Cembrano, Gabriela; Puig, Vicenç

https://doi.org/10.1016/j.conengprac.2021.104900

Control Engineering Practice 115 (2021) 104900

Contents lists available at ScienceDirect

Control Engineering Practice

journal homepage: www.elsevier.com/locate/conengprac

Chance-constrained stochastic MPC of Astlingen urban drainage benchmark network☆

Jan Lorenz Svensen [a,*], Congcong Sun [b,c], Gabriela Cembrano [b,d], Vicenç Puig [b]

[a] Department of Applied Mathematics and Computer Science, Technical University of Denmark, Richard Petersens Plads 324, 2800 Kongens Lyngby, Denmark
[b] Advanced Control Systems Group, the Institut de Robòtica i Informàtica Industrial (CSIC-UPC), Llorens i Artigas, 4-6, 08028 Barcelona, Spain
[c] Farm Technology Group, Wageningen University, Wageningen, 6700 AA, The Netherlands
[d] CETaqua, Water Technology Centre, Barcelona, 08904, Spain

ARTICLE INFO

Keywords:
Astlingen benchmark network
CSO
Stochastic MPC
Chance-Constrained
Real-Time Control

ABSTRACT

In urban drainage systems (UDS), a proven method for reducing the combined sewer overflow (CSO) pollution is real-time control (RTC) based on model predictive control (MPC). MPC methodologies for RTC of UDSs in the literature rely on the computation of the optimal control strategies based on deterministic rain forecast. However, in reality, uncertainties exist in rainfall forecasts which affect severely accuracy of computing the optimal control strategies. Under this context, this work aims to focus on the uncertainty associated with the rainfall forecasting and its effects. One option is to use stochastic information about the rain events in the controller; in the case of using MPC methods, the class called stochastic MPC is available, including several approaches such as the chance-constrained MPC(CC-MPC) method. In this study, we apply CC-MPC to the UDS. Moreover, we also compare the operational behavior of both the classical MPC with perfect forecast and the CC-MPC based on different stochastic scenarios of the rain forecast. The application and comparison have been based on simulations using a SWMM model of the Astlingen urban drainage benchmark network. From the simulations, it was found that CSO volumes were larger when CC-MPC had overestimating forecast biases, while for MPC they increased with any presence of forecast biases.

1. Introduction

The state-of-the-art during the last couple of decades, regarding the operation of urban drainage systems (UDS), has seen Model Predictive Control (MPC) (Maciejowski, 2002) been proved beneficial for achieving optimal operation of the UDS (Cen & Xi, 2009; Gelormino & Ricker, 1994; Halvgaard & Falk, 2017; Marinaki & Papageorgiou, 2005; Ocampo-Martinez, 2010; Sun, Joseph, Cembrano, Puig and Meseguer, 2018; Sun et al., 2017, 2020; Svensen, Niemann, & Poulsen, 2019). While these studies have used different types of modeling and optimization techniques to compute the best control actions; MPC applications of UDS has predominately been assumed to be deterministic, including the rain forecast (Cembrano et al., 2004; Cen & Xi, 2009; Gelormino & Ricker, 1994; Halvgaard & Falk, 2017; Joseph-Duran, Meseguer, Cembrano, & Maruejouls, 2017; Marinaki & Papageorgiou, 2005; Ocampo-Martinez, 2010; Overloop, 2006; Sun, Cembrano, Puig and Meseguer, 2018; Sun, Joseph et al., 2018, 2017; Sun et al., 2017; Sun, Puig and Cembrano, 2020; Sun, Svensen et al., 2020; Svensen et al., 2019). This in spite of models and forecasts are subject to uncertainty, and may risk in introducing sub-optimal or undesired behaviors to the MPC solutions. For a more realistic scenario, uncertainty has to be considered as a part of the UDS. The way how the uncertainty is treated by the control, becomes an important design decision: using a stochastic approach, or robustly operating on worst-case assumptions.

1.1. Literature

While the basic formulation of MPC is deterministic and does not consider uncertainty at all; how to handle uncertainty in MPC has been researched for many years (Arellano-Garcia & Wozny, 2009; Dhar & Datta, 2006; Evans, Cannon, & Kouvaritakis, 2012; Garatti, Campi, Garatti, & Prandini, 2009; Grosso, Ocampo-Martinez, Puig, & Joseph-Duran, 2014; Kouvaritakis & Cannon, 2016; Magni, De Nicolao, Scattolini, & Allgöwer, 2003; Mesbah, 2016; Sun, Dai, Liu, Xia and Johansson, 2018; Svensen, Niemann, Falk, & Poulsen, 2021; Wan & Kothare, 2002). This has resulted in several different methods for handling uncertainty divided into two categories; the group of the methods known collectively as robust MPC (Kouvaritakis & Cannon, 2016; Magni et al., 2003; Sun, Dai et al., 2018; Wan & Kothare, 2002),

☆ This document is the results of the research project funded by the Spanish State Research Agency through the María de Maeztu Seal of Excellence to IRI (MDM-2016-0656), internal project of TWINs, and also supported by Innovation Fond Denmark through the Water Smart City project (project 5157-00009B).
* Corresponding author.
E-mail addresses: jlsv@dtu.dk (J.L. Svensen), congcong.sun@upc.edu (C. Sun), gabriela.cembrano@upc.edu (G. Cembrano), vicenc.puig@upc.edu (V. Puig).

https://doi.org/10.1016/j.conengprac.2021.104900
Received 28 August 2020; Received in revised form 1 April 2021; Accepted 15 July 2021
Available online xxxx
0967-0661/

and the group known as stochastic MPC (Arellano-Garcia & Wozny, 2009; Dhar & Datta, 2006; Evans et al., 2012; Garatti et al., 2009; Grosso et al., 2014; Kouvaritakis & Cannon, 2016; Mesbah, 2016; Svensen et al., 2021).

The first group essentially considers the worst-case scenario and operates conservatively so that the solution is optimal for all possible realizations of the uncertainty. The second group addresses the uncertainty by using knowledge about the uncertainty (Mesbah, 2016), such as its distribution to only take the statistical likely scenarios into account for the control.

In this work, we will focus on a method from the group of stochastic methods known as chance-constrained MPC (CC-MPC) (Arellano-Garcia & Wozny, 2009; Dhar & Datta, 2006; Grosso et al., 2014; Svensen et al., 2021) to operate the UDS in order to reduce pollution to the receiving waters through minimization of the combined sewer overflows (CSO). Given that the CSOs are purely dependent on the volumes and flows of the system; the overflow constraints are intrinsically feasible and probabilistic insensitive, when CC-MPC is applied directly. We will therefore use the revised CC-MPC formulation (Svensen et al., 2021) in this work.

Stability of MPC is an important issue since local optimization in a finite horizon does not always guarantee stability (Lee, Wang, & Tan, 1996). The most widely approach to guarantee stability in MPC approach is adding equality constraint on the final state in the prediction horizon (Genceli & Nikolaou, 1993; Nicolao, Magni, & Scattolini, 1998), which is used in important classical MPC problems, such as tracking MPC. However, in this paper, the MPC optimize specific objective functions instead of tracking a defined trajectory. Also given that UDSs are intrinsically stable in reality and in models, water cannot be generated, we will leave the stability of CC-MPC as future research.

In a previous of authors' work (Sun, Svensen et al., 2020), we obtained good results implementing a deterministic MPC in the Astlingen network regarding minimizing the CSO volume of the system and maximizing the amount of treated wastewater by the wastewater treatment plant (WWTP), in comparison with other real-time control strategies.

The Astlingen network is a benchmark urban drainage network which has been designed by the German Water Association (DWA) complementing the German DWA-M180 document on planning of RTC (real-time control) systems (DWA, 2005). This benchmark model has been used widely and proven sufficient enough to represent a realistic urban drainage network (Schütze, Lange, Pabst, & Haas, 2018). Moreover, the Storm Water Management Model (SWMM), the simulation platform used for validating MPC control of Astlingen network, is a high-fidelity simulation software, which can present detailed hydrodynamics of the urban drainage network in a virtual reality way (Rossman, 2015). So that, the benchmark Astlingen network based on SWMM can work well as a realistic system.

1.2. Main contribution

Our contribution in this paper is the application and implementation of the stochastic CC-MPC method in a high-fidelity simulation of the Astlingen system. In the research, the usage of CC-MPC in the application of UDS is sparse at best, and to our knowledge a first using high-fidelity simulations for validation. In our implementation, we will consider the uncertainty to be in the rainfall forecast. We will provide a comparison of the performance of the CC-MPC with that of an deterministic MPC with a perfect forecast and under different scenarios of the uncertainty. The key performance indexes considered are the CSO volume, and the volume received by the WWTP.

The following sections of the paper are dedicated to the internal MPC model, the MPC design, and the results of the simulation respectively.

1.3. Notation

In this paper, the following mathematical notations are used. $\overline{f}$ indicates the maximum of a given function $f(x)$, β represents the volume-flow coefficient (Singh, 1988), and bold font is used to indicate vectors. The formulation $\|\mathbf{x}\|_A^2 = \mathbf{x}^T A\mathbf{x}$ is the weighted quadratic norm of x. The superscript u indicates control variables, superscript w indicates CSO elements, and the superscripts *in* and *out* indicate inflow and outflow related flow, respectively. The letters V and q indicate variables of volume and flow respectively, while the variables written with w are inflows from catchments. The notation ΔT and the subscript k represent the sampling time and the sample number.

2. Internal model of the Astlingen benchmark network

The Astlingen urban drainage network consists of six tanks and a single outflow towards a WWTP (see Fig. 1). In between and upstream of the tanks there are pipes of varying lengths, causing flow delays in the system, between 5 and 20 min delays. The system also consists of four pipes with CSO capabilities. The control variables of the system are the outflow of tanks 2, 3, 4, and 6. The desired operation of the system is to have the least amount of CSO as possible, and secondly having the largest amount of wastewater being sent to the WWTP. For designing an MPC controller for the system, an internal model describing the dynamics and constraints of this system is required, typically a simplified model of the system capturing the main dynamic behaviors is used.

From Fig. 1, it is clear that the system can be deduced to be uncontrollable (passive) in the sections upstream the tanks; therefore, the internal model will be limited to only covering the tanks of the system. The internal model is constructed with the same modular approach as used in previous works (Sun, Svensen et al., 2020), and using a sampling time ΔT of 5 min. In the internal model, the CSO are treated as optimization variables through a penalty approach (Halvgaard & Falk, 2017). The elements of the internal model consist of the following parts: linear reservoir tanks and pipes with delays that are described below.

In CC-MPC, the internal model includes the uncertainties. The constraints are reformulated as either as the expectation of the constraints or as a probabilistic constraints with a chosen probability of being true. The prior is in general used for equality constraints, while the latter is used for inequality constraints. The probabilistic constraints are introduced to constrict the deterministic constraints, to statistically avoid undesired behaviors such as the controller attempting to draw water from en empty tank, due to the uncertain volume information. The constriction is obtained by using quantiles to provide a deterministic version of the probabilistic constraints.

In this work, the only sources of uncertainty considered is the runoff inflows w generated by forecasted rainfalls, covering runoff from catchments and passive flows from upstream sections. We will assume the uncertainty follows a truncated normal distribution, given that rainfalls cant be negative and are upperbounded by physics, water caring capacity of clouds. The normal distribution is commonly used to interpret fluctuations in measured or forecasted variables (Karantonis & Weber, 2016; Scott, 2003).

For linear models with uncertainties following a truncated normal distribution, the uncertainties undergoes a linear transformations into corresponding truncated normal distributions, see Appendix A, before being summed. Unfortunately, the sum of truncated Normals are not itself a truncated Normal (Horrace, 2005) Appendix B, but can be approximated as a truncated normal distribution for the usage of probabilistic constraints, see Appendix C. The probabilistic constraints can then be written deterministically as shown in (1). The deterministic part x includes the optimizable variables and the stochastic part X lies in the interval $[a, b]$, with the expectation $E\{X\}$ and standard deviation $\sigma\{X\}$, and $\Phi^{-1}(\Gamma)$ is the quantile function of the standard normal distribution

$$Pr(X \leq x) \geq \gamma \Leftrightarrow x \geq E\{X\} + \sigma\{X\}\Phi^{-1}(\Gamma) \tag{1}$$

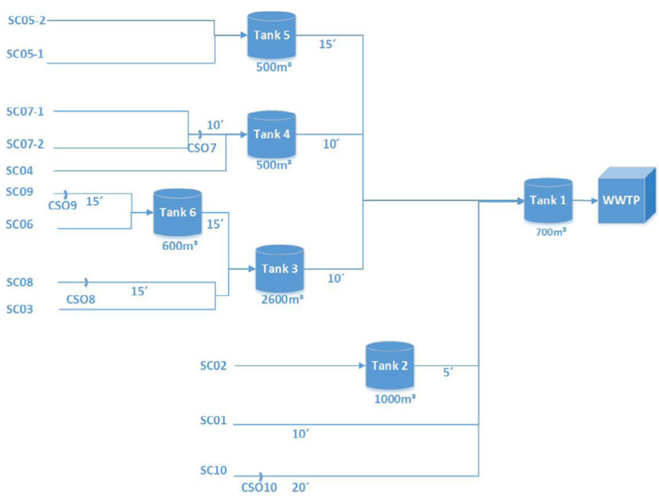

Fig. 1. A scheme of the Astlingen Benchmark Network (Schütze et al., 2018) showing the interconnections between tanks, pipes and the WWTP, with CSOs coming from the six tanks and the four pipes noted CSO7 to CSO10. The delay between tanks and/or pipes are noted by x' in minutes.

$$\Gamma = \gamma\Phi\left\{\frac{b-E\{X\}}{\sigma\{X\}}\right\} + (1-\gamma)\Phi\left\{\frac{a-E\{X\}}{\sigma\{X\}}\right\} \tag{2}$$

where Γ is the truncated version of the desired probability confidence level γ.

The probabilistic constraints can therefore be described using process equations of the expectations and variances of the dynamics of each element. It is assumed that the different sources of uncertainties are independently distributed, in both spatial and temporal sense.

For simplicity of notation, the following formulations of each module is given for the non-truncated case $\Gamma = \gamma$. The formulation of the Γ of each corresponding constraint can be obtain from the iterations of the process equations; for the corresponding expectations and variances of the constraint.

2.1. Linear reservoir tank — passive outflow

The linear reservoir model has either a passive outflow or a controlled outflow and is based on mass-balance to describe the dynamics of tank volume. The volume of the tank V_k is driven by the inflow q_k^{in} and the weir overflow q_k^{w}. In the case of passive outflows, the outflow is controlled by gravity, and is assumed linear with a volume-flow coefficient (Singh, 1988) defined as $\beta = \overline{q}^{out}/\overline{V}$.

For the passive outflow case, the volume update and the outflow are defined by:

$$V_{k+1} = (1-\Delta T\beta)V_k + \Delta T(q_k^{in} - q_k^{w}) \tag{3}$$

$$q_k^{out} = \beta V_k \tag{4}$$

The constraints of the reservoir are based on the physical constraints with the tank limits given by

$$0 \le (1-\Delta T\beta)V_k + \Delta T(q_k^{in} - q_k^{w}) \le \overline{V} \tag{5}$$

$$0 \le q_k^{w} \tag{6}$$

2.1.1. CC-MPC formulation — passive tank

Utilizing the revised CC-MPC formulation (Svensen et al., 2021) mentioned earlier, the passive reservoir model can be reformulated, such that the volume update and the outflow are defined by their expectation and variance given by

$$E\{V_{k+1}\} = (1-\Delta T\beta)E\{V_k\} + \Delta T(E\{q_k^{in}\} - q_k^{w}) \tag{7}$$

$$E\{q_k^{out}\} = \beta E\{V_k\} \tag{8}$$

$$\sigma^2\{V_{k+1}\} = (1-\Delta T\beta)^2\sigma^2\{V_k\} + \Delta T^2\sigma^2\{q_k^{in}\} \tag{9}$$

$$\sigma^2\{q_k^{out}\} = \beta^2\sigma^2\{V_k\} \tag{10}$$

The stochastic interpretation of the physical constraints is given by (11)–(15), utilizing slack variables for guaranteeing feasibility (Svensen et al., 2021).

The stochastic constraint for the lower limit of the tank is given by (11), while the upper limit is given by (12) and (13). The first one is a stochastic constraint for avoiding weir overflow q_k^{w}, while the latter is an expectation constraint defining the expected overflow

$$\sigma\{(1-\Delta T\beta)V_k + \Delta T q_k^{in}\}\Phi^{-1}(\gamma) - s_k \le (1-\Delta T\beta)E\{V_k\} + \Delta T(E\{q_k^{in}\} - q_k^{w}) \tag{11}$$

$$(1-\Delta T\beta)E\{V_k\} + \Delta T E\{q_k^{in}\} \le \overline{V} - \sigma\{(1-\Delta T\beta)V_k + \Delta T q_k^{in}\}\Phi^{-1}(\gamma) + c_k \tag{12}$$

$$(1-\Delta T\beta)E\{V_k\} + \Delta T(E\{q_k^{in}\} - q_k^{w}) \le \overline{V} \tag{13}$$

$$s_k \le \sigma\{(1-\Delta T\beta)V_k + \Delta T q_k^{in}\}\Phi^{-1}(\gamma) \tag{14}$$

$$0 \le q_k^{w}, s_k, c_k \tag{15}$$

The limits on the slack variables s_k, c_k are given by (14) and (15). For the control of the Astlingen model, Tank 1 and Tank 5 are considered tanks with passive outflow.

2.2. Linear reservoir tank — Controlled outflow

For a linear reservoir tank with controlled outflow, the volume is driven by the inflow q_k^{in}, the control flow q_k^{u} and the weir overflow q_k^{w}. The volume update and outflow are defined by

$$V_{k+1} = V_k + \Delta T(q_k^{in} - q_k^{u} - q_k^{w}) \tag{16}$$

$$q_k^{out} = q_k^{u} \tag{17}$$

and the physical limits on the tanks are given by

$$0 \le V_k + \Delta T(q_k^{in} - q_k^{u} - q_k^{w}) \le \overline{V} \tag{18}$$

The limits of the control including two upper limits of the control flow are defined as

$$0 \le q_k^{u} \le \overline{q}^{u} \tag{19}$$

$$q_k^{u} \le \beta V_k \tag{20}$$

$$0 \le q_k^{w} \tag{21}$$

where the first one establishes the physical limit of the outflow pipe, and the other one a linear Bernoulli expression given by the volume-flow coefficient β.

2.2.1. CC-MPC formulation — Controlled tank

The controlled reservoir model can be formulated for CC-MPC as below, considering that the volume update and outflow are defined by the expectation and variance

$$E\{V_{k+1}\} = E\{V_k\} + \Delta T(E\{q_k^{in}\} - q_k^{u} - q_k^{w}) \tag{22}$$

$$E\{q_k^{out}\} = q_k^{u} \tag{23}$$

$$\sigma^2\{V_{k+1}\} = \sigma^2\{V_k\} + \Delta T^2\sigma^2\{q_k^{in}\} \tag{24}$$

$$\sigma^2\{q_k^{out}\} = 0 \tag{25}$$

Note that the outflow variance is zero, due to the control.

According to the reformulation (Svensen et al., 2021), the stochastic version of the physical constraints is given by

$$0 \le E\{V_k\} + \Delta T(E\{q_k^{in}\} - q_k^{u} - q_k^{w}) \tag{26}$$

$$E\{V_k\} + \Delta T(E\{q_k^{in}\} - q_k^{u}) \le \overline{V} - \sigma\{V_k + \Delta T q_k^{in}\}\Phi^{-1}(\gamma) + c_k \tag{27}$$

$$E\{V_k\} + \Delta T(E\{q_k^{in}\} - q_k^{u} - q_k^{w}) \le \overline{V} \tag{28}$$

$$0 \leq q_k^u \leq q^u \tag{29}$$

$$q_k^u \leq \beta E\{V_k\} - \beta\sigma\{V_k\}\Phi^{-1}(\gamma) + s_k \tag{30}$$

$$s_k \leq \beta\sigma\{V_k\}\Phi^{-1}(\gamma) \tag{31}$$

$$0 \leq q_k^w, c_k, s_k \tag{32}$$

where the slack variables are limited by (31) and (32). The constraints (26)–(28) define the upper and lower limits of the tank, in a similar way as (11)–(13). The control limits are defined by (29) and (30).

2.2.2. Decoupling of slack variables

In (26), the lower limit of the tank is given as expectation constraint, while in (11) it was expressed in a probabilistic manner. The change is due to the interconnections of the slack variables of the upper and lower constraints as follows

$$s_k \leq c_k + \overline{V} - \Delta T q_k^w \tag{33}$$

where the upper slack is forced to be active if the lower slack is too large.

This can lead to an undesired trade-off during optimization when the uncertainty term is too large. This can be solved by a rescaling of the optimization weights or by reformulating the probability constraint. The latter was used here. The probability of the tank volume being above zero (34) can be rewritten

$$\begin{aligned} &Pr(0 \leq V_k + \Delta T(q_k^{in} - q_k^u - q_k^w)) \\ &= Pr(\Delta T q_k^u \leq V_k + \Delta T(q_k^{in} - q_k^w)) \geq \gamma \end{aligned} \tag{34}$$

by considering that the tank volume V_k is always below the upper tank limit, given that any volume above it would have turned into an overflow. This leads to the volume only decreases, when the control flow is used, i.e.

$$V_k \leq V_k + \Delta T(q_k^{in} - q_k^w) \tag{35}$$

From here, we can replace (34) with a stricter and simpler probability as follows

$$Pr(0 \leq V_k + \Delta T(q_k^{in} - q_k^u - q_k^w)) \geq Pr(\Delta T q_k^u \leq V_k) \geq \gamma \tag{36}$$

By multiplying with the volume-flow coefficient β and assuming that $\beta \Delta T \leq 1$, the probability constraint can be rewritten even stricter. The assumption is fair, given that if the opposite is true, then the volume can become negative. The resulting probability constraint

$$Pr(\beta \Delta T q_k^u \leq \beta V_k) \geq Pr(q_k^u \leq \beta V_k) \geq \gamma \tag{37}$$

can be recognized as (30), the stochastic version of one of the upper control limits. This indicates that if (30) holds so does (37), and therefore (34) would be a duplicate. For this reason, (34) can be replaced with the expectation constraint given in (26), for the inclusion of the lower limit of the tank.

2.3. Pipe with delays

In the Astlingen network (Schütze et al., 2018), the tanks and upstream catchments are connected through pipes. The presence of these pipes introduces delays in the flows to the tanks from the upstream parts of the system. The importance of these delays depend on the chosen sampling time. Delays η of exactly one sampling can be described by

$$\eta_{k+1,i} = q_{k,i}^{in} \tag{38}$$

$$q_{k,i}^{out} = \eta_{k,i} \tag{39}$$

Delays of multiple sampling times, can be constructed as a cascade of single delays as seen in Table 1. The $\eta_{1:5}$, $\eta_{1:10}$ and $\eta_{1:15}$ delay states are the delayed flows to Tank 1 for 5, 10 and 15 min delays respectively.

Table 1
Inflows to the different elements of the systems.

Subpart	Inflow	Subpart	Inflow
T_1	$q_{k,\eta_{1:5}}^{out}$	$\eta_{1:5}$	$q_{k,T_2}^{out} + q_{k,\eta_{1:10}}^{out}$
T_2	$w_{k,2}$	$\eta_{1:10}$	$w_{k,1} + q_{k,T_2}^{out} + q_{k,T_4}^{out} + q_{k,\eta_{1:15}}^{out}$
T_3	$w_{k,3} + q_{k,\eta_{3:5}}^{out}$	$\eta_{1:15}$	q_{k,T_5}^{out}
T_4	$w_{k,4}$	$\eta_{3:5}$	$q_{k,\eta_{3:10}}^{out}$
T_5	$w_{k,5}$	$\eta_{3:10}$	$q_{k,\eta_{3:15}}^{out}$
T_6	$w_{k,6}$	$\eta_{3:15}$	q_{k,T_6}^{out}

2.3.1. CC-MPC formulation — Delays

For the CC-MPC, the delay equations are replaced by their expectations

$$E\{\eta_{k+1,i}\} = E\{q_{k,i}^{in}\} \tag{40}$$

$$E\{q_{k,i}^{out}\} = E\{\eta_{k,i}\} \tag{41}$$

In addition, the variance of the delay equations are given by

$$\sigma^2\{\eta_{k+1,i}\} = \sigma^2\{q_{k,i}^{in}\} \tag{42}$$

$$\sigma^2\{q_{k,i}^{out}\} = \sigma^2\{\eta_{k,i}\} \tag{43}$$

2.4. Constructing the model

The MPC model of Astlingen network can now be constructed considering the interconnection of the tanks and delays presented in Fig. 1 and using the models discussed above. The inflow of each considered subpart of the network are summarized in Table 1. The ith tank and the delay flow to it are noted by T_i and $\eta_{i:j}$, respectively, with j being the remaining delay in minutes to the tank. The outflow of subpart z is written as $q_{k,z}^{out}$, and the ith run-off inflow to the system is given by $w_{k,i}$.

3. MPC design

The design of controllers used in this work for both MPC and CC-MPC are based on the models discussed above and the minimization of a cost that considers the following operational objectives for the network:

- Maximizing flow to the WWTP
- Minimizing flow to the river/creek
- Minimizing roughness of control

The first objective can be achieved by a linear negative cost on the outflow of tank 1, while the second objective can be formulated as a linear positive cost on the total overflow of the system; these objectives are collectively written as $\mathbf{z}_k$, with the weight $\mathbf{Q}$. The third objective can be written as a quadratic cost on the change in control flow Δq_k^u, with the diagonal weight R. Due to the overflow being modeled by a penalty approach, a fourth objective of minimizing the accumulated overflow volume $\mathbf{V}_k^w$ is introduced, with the weight $\mathbf{W}$.

$$J = \min_{\mathbf{q}^u, \mathbf{q}^w} \Sigma_{k=0}^{N} \|\Delta \mathbf{q}_k^u\|_R^2 + \mathbf{Q}^T \mathbf{z}_k + \mathbf{W}^T \mathbf{V}_k^w \tag{44}$$

subject to

$$\mathbf{z} = \Phi_{Con}\mathbf{q}^u + \Psi \mathbf{V}_0 + \Theta \mathbf{w} + \Gamma \mathbf{q}^w \tag{45}$$

$$\mathbf{V}_k^w = \Sigma_{i=0}^{k} \Delta T \mathbf{q}_i^w \tag{46}$$

By using the MPC model over the prediction horizon N, the cost function of the MPC can be written as in (44), while the predicted objectives $\mathbf{z}$ and accumulated overflow volumes, given by (45) and (46), are derived by substitution of the predicted volumes and delays.

Table 2
Cost function weighting of accumulated overflow volume **W**, showing a higher cost for upstream elements.

T1	T2	T3	T4	T5	T6
1000	5000	5000	5000	5000	10 000

The constraints of the MPC model can similarly be collected into a single matrix inequality given by

$$\Omega_{Con}\mathbf{q}^u + \Omega_{vol}\mathbf{V}_0 + \Omega_{rain}\mathbf{w} + \Omega_{weir}\mathbf{q}^w \leq \boldsymbol{\Omega} \tag{47}$$

where the subscripts of the Ω matrix terms relates to the corresponding terms: Con for the control term, vol for the initial volume term, $rain$ for the external inflows term, and $weir$ for the term describing the CSOs of the system.

The design of the CC-MPC can similarly be derived using the corresponding model presented above. The cost of the resulting optimization program, appear as the expectation of (44) with the added linear cost term of the minimization of the slack variables $\mathbf{c}$ and $\mathbf{s}$ with weights $\mathbf{W}_c$ and $\mathbf{W}_s$

$$J = \min_{\mathbf{q}^u,\mathbf{q}^w,\mathbf{c},\mathbf{s}} E\{\Sigma_{k=0}^N \|\Delta\mathbf{q}_k^u\|_R^2 + \mathbf{Q}^T\mathbf{z}_k + \mathbf{W}^T\mathbf{V}_k^w\} + \mathbf{W}_c^T\mathbf{c} + \mathbf{W}_s^T\mathbf{s} \tag{48}$$

The expected objectives are given by

$$E\{\mathbf{z}\} = \Phi_{Con}\mathbf{q}^u + \Psi E\{\mathbf{V}_0\} + \Theta E\{\mathbf{w}\} + \Gamma\mathbf{q}^w \tag{49}$$

while the accumulated overflow volume is unchanged from (46).

The matrix inequality of the collected probabilistic constraints are given by

$$\begin{aligned}&\Omega_{Con}\mathbf{q}^u + \Omega_{vol}E\{\mathbf{V}_0\} + \Omega_{rain}E\{\mathbf{w}\} + \Omega_{weir}\mathbf{q}^w \leq \\ &\quad \boldsymbol{\Omega} - \sigma\{\Omega_{vol}\mathbf{V}_0 + \Omega_{rain}\mathbf{w}\}\Phi^{-1}(\gamma) + \Omega_s\mathbf{s} + \Omega_c\mathbf{c}\end{aligned} \tag{50}$$

and the variance term

$$\sigma^2\{\Omega_{vol}\mathbf{V}_0 + \Omega_{rain}\mathbf{w}\} = \Xi_{vol}\sigma^2\{\mathbf{V}_0\} + \Xi_{rain}\sigma^2\{\mathbf{w}\} \tag{51}$$

The weighting of the different objectives in the cost functions is done in accordance with the penalty approach (Halvgaard & Falk, 2017; Svensen et al., 2019). The priority of the different objectives is given in the following order from highest to lowest priority:

1. Minimization of accumulated overflow volume $\mathbf{V}_k^w$
2. Minimization of flow to the river/creek
3. Maximizing flow to the WWTP
4. Minimizing roughness of control

The weightings used in this work are for the accumulated overflow volume given in Table 2 for each tank weir. The weights of the remaining objectives are 2 for the flow to the river/creek, −1 for the flow to the WWTP, 0.01 for the roughness of the control, and in the CC-MPC case 10 for the usage of the slack variables. The weights indicate that the avoidance of the flow to the river is prioritized twice as high as increasing flow to the WWTP. The weight on the roughness indicates the desire for the control to be smooth, but not a general priority. As seen from the table, the priority of the accumulated overflow is significantly higher than the other objectives. With the cost for upstream tanks being higher than downstream tanks, to avoid nonphysical overflow predictions (Halvgaard & Falk, 2017; Svensen et al., 2019).

4. Results

The CC-MPC discussed above has been applied to the SWMM model of the Astlingen benchmark network (Sun, Svensen et al., 2020). In order to evaluate the performance of the CC-MPC, and its response to different types of uncertainties, we have ran simulation series with four different scenarios. Each scenario were quantified by a parameter, which were the only varied in its own simulation series; in order for the effect of the given parameter to be clear.

Table 3
Overflow results of the SWMM simulations with different controllers: MPC, and CC-MPC with the probability guarantees of 100–60%.

Tank & Pipes	MPC	CC-MPC 100%	CC-MPC 90%	CC-MPC 80%	CC-MPC 70%	CC-MPC 60%
T1	93 251	93 713	92 927	93 015	93 114	93 229
T2	15 484	15 683	15 544	15 543	15 543	15 543
T3	34 017	34 174	34 313	34 214	34 427	34 248
T4	4 814	4 823	4 814	4 814	4 814	4 815
T5	15 147	15 147	15 147	15 147	15 147	15 147
T6	37 950	37 723	37 946	37 939	37 980	37 870
P7	4 016	4 016	4 015	4 016	4 016	4 016
P8	16 207	16 207	16 191	16 203	16 203	16 199
P9	4 030	4 030	4 029	4 029	4 029	4 029
P10	4 838	4 838	4 842	4 839	4 839	4 840
River	183 754	184 585	183 778	183 774	184 086	184 020
Creek	45 996	45 769	45 990	45 984	46 025	45 915
Total	229 750	230 353	229 768	229 758	230 111	229 935
R. %		−0.4522%	−0.0131%	−0.0109%	−0.1807%	−0.1448%
C. %		0.4935%	0.0130%	0.0261%	−0.0630%	0.1761%
Tot. %		−0.2625%	−0.0078%	−0.0035%	−0.1571%	−0.0805%

The first scenario were variations in the probability confidence level γ, change from 60% to 100%. The second scenario considers the bound on the uncertainty, while the third and fourth scenarios affects the expectation of the inflow forecasts; deviating it from the actual inflow, using scaled and offset biases respectively. The base value of each parameter in the simulations were: a 90% probability confidence level, a 50% uncertainty bound, 0% scaled bias and zero offset bias.

In all the simulations, the uncertainty has been assumed that it follows a truncated normal distribution, where the lower bound is zero and the upper bound is three standard deviations above the expected disturbance.

For the evaluation of the results, we compare with the results of simulations with the deterministic MPC with perfect forecasts, in order to provide an indication of the expected performance if one knows the exact future within the prediction horizon. A 100 min prediction horizon were chosen, so that the delays of the systems were covered, and the computation of MPC would not have numerical issues. For the actual rainfall in simulations, a continuous historic long-term rainfall series of 1 year with a time resolution of 5 min provided by the Erftverband Water Association are used. Together with spatially distributed rainfall input and realistic boundary conditions, the rainfall data can represent a benchmark simulation and control example. The use of historic data can avoid uncertainties incurred by synthetically generated rainfall data (Müller, Schütze, & Bárdossy, 2007).

4.1. CC-MPC with various probability confidence levels γ

The results in terms of CSO volume from varying the probability confidence level can be observed in Table 3, and in Table 4 for the volume of treated water in WWTP. From these tables, we can see the distribution of CSO through the system. Both the CSO and WWTP volume of the CC-MPCs are comparatively close to the results of the deterministic MPC, regardless of the chosen probability guarantee. Similar conclusions can be obtained from Fig. 2, which presents volume dynamics for the tanks with controllable orifices (Tank 2, Tank 3, Tank 4, Tank 6) under CC-MPCs with probability confidence levels in the range from 60% to 100%. In Fig. 2, there are small deviations for the tank volumes resulting from CC-MPCs with different probability confidence levels. However, a slightly trend can be observed such that the smaller the probability confidence levels, the larger volumes at the peak points, which may reach the maximal storage more easily and generate more CSOs for the corresponding tanks. This figure only presents simulation results for day 10 and day 11 in order to provide a clearer view.

Table 4
Treated wastewater results of the SWMM simulations with different controllers: MPC, and CC-MPC with the probability guarantees of 100–60%.

	MPC	CC-MPC 100%	CC-MPC 90%	CC-MPC 80%	CC-MPC 70%	CC-MPC 60%
WWTP Vol.	3 772 057	3 771 560	3 772 159	3 772 088	3 771 889	3 771 795
Imp. %		−0.0132%	0.0027%	0.0008%	−0.0045%	−0.0069%

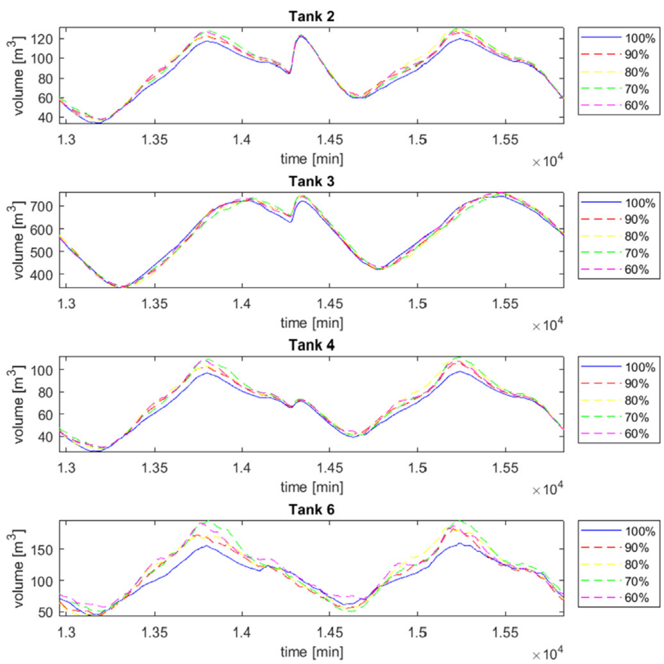

Fig. 2. The volumes for the tanks with controllable orifices (Tank 2, Tank 3, Tank 4, Tank 6) for the CC-MPCs with probability confidence levels γ of 100%–60%.

4.2. CC-MPC with various uncertainty bounds

The uncertainty bound describes the interval the uncertainty can take. For these simulations, a constant lower bound of zero is used; while the upper bound is defined as a percentage p of the actual inflow above the expected rain inflow, see (52). The standard deviation of the uncertainty is assumed a third of the actual rain inflow times the percentage p. For normal distributions, this leads to the bound to be defined as

$$bound = [0, E\{q\} + pq^{actual}] \tag{52}$$

corresponding to the 99.7% confidence interval of a corresponding unbounded distribution, if expectation matches the actual inflow. The CC-MPC is tested with percentage p bounds of 25%, 50% and 75%. From Tables 5 and 6, we can observe the resulting CSO volume and WWTP volume, respectively. It can be observed that the deviations from the results of the deterministic MPC are negligible of up to a few hundred cubic meters. Fig. 3 provides detailed dynamic evolution for the tank volumes of CC-MPC with uncertainty bounds of 25%, 50% and 75%, confirming conclusions obtained from Table 5 showing that the deviations brought by CC-MPCs are negligible. On the other hand, it can be observed from Fig. 3 that, the larger the uncertainty bound is, the smaller the tank volume is, which may cause less CSOs to the corresponding tank. This is because the larger uncertainty bounds make the CC-MPC generate more conservative orifice operations with the function of preventing CSOs. This conclusion is also in agreement with the basic deviations trends for the tanks CSO comparisons in Table 5.

Table 5
Overflow results of the SWMM simulations with different controllers: MPC and CC-MPC with the uncertainty bound of 25%–75%.

Tank & Pipes	MPC	CC-MPC 25%	CC-MPC 50%	CC-MPC 75%
T1	93 251	93 067	92 927	92 795
T2	15 484	15 543	15 544	15 544
T3	34 017	34 267	34 313	34 067
T4	4 814	4 814	4 814	4 814
T5	15 147	15 147	15 147	15 147
T6	37 950	37 939	37 946	37 673
P7	4 016	4 016	4 015	4 016
P8	16 207	16 203	16 191	16 207
P9	4 030	4 029	4 029	4 030
P10	4 838	4 839	4 842	4 838
River	183 754	183 879	183 778	183 412
Creek	45 996	45 984	45 990	45 718
Total	229 750	229 864	229 768	229 130
R. %		−0.0680%	−0.0131%	0.1861%
C. %		0.0261%	0.0130%	0.6044%
Tot. %		−0.0496%	−0.0078%	0.2699%

Table 6
Treated wastewater results of the SWMM simulations with different controllers: MPC, and CC-MPC with the uncertainty bound of 25%–75%.

	MPC	CC-MPC 25%	CC-MPC 50%	CC-MPC 75%
WWTP Vol.	3 772 057	3 772 086	3 772 159	3 772 676
Imp. %		0.0008%	0.0027%	0.0164%

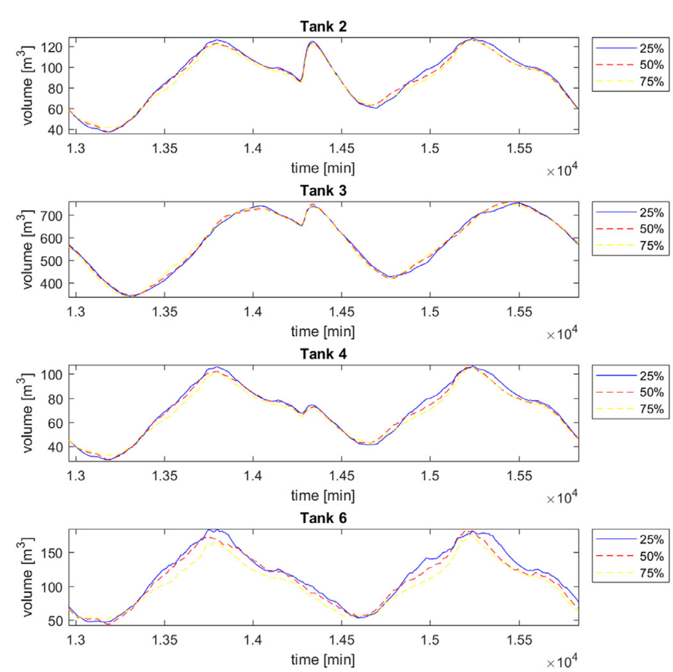

Fig. 3. The volumes for the tanks with controllable orifices (Tank 2, Tank 3, Tank 4, Tank 6) for the CC-MPC with the uncertainty bound of 25–75%.

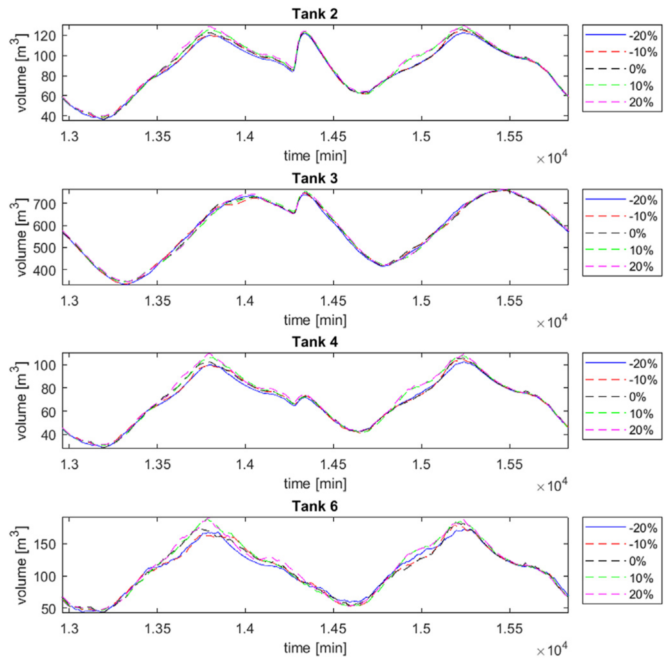

Fig. 4. The volumes for the controllable tanks under CC-MPC with different scaled bias.

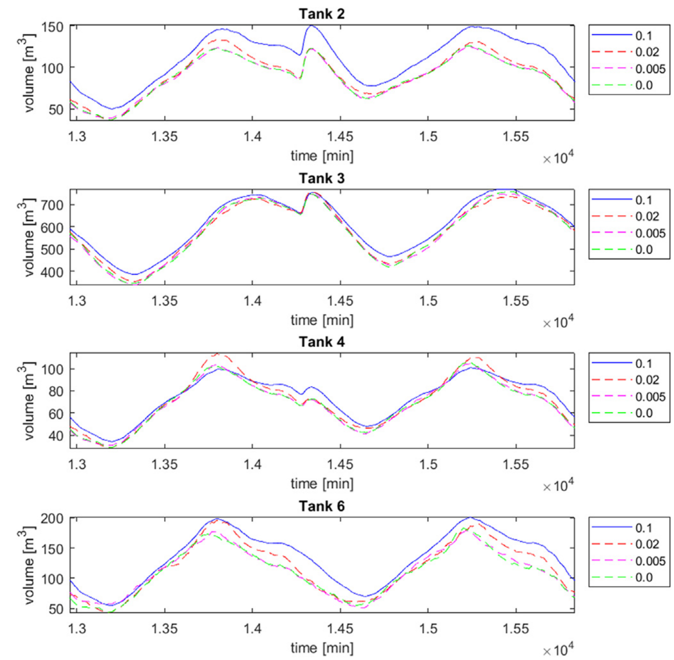

Fig. 5. The volumes for the controllable tanks under CC-MPC using different offsets.

4.3. CC-MPC with various scaled biases

In this section, the percentage bound on the uncertainty are kept constant, 50%, instead the expected inflow is introduced as a scaled version of the actual rain inflow, given by

$$E\{q\} = aq^{actual} \tag{53}$$

Both the CC-MPC and the MPC are tested with 20% and 10% underestimated inflow, perfect forecast, and 10% and 20% overestimated inflow. The results can be seen in Tables 7 and 8, for the CSO volume and the WWTP volume, respectively. We can observe that if the expected inflow is overestimated then both types of MPC perform relatively worse as the overestimation increases with respect to CSO volume, and slight improvement of WWTP volume. When the inflow is underestimated, then the MPC performs significantly worse than the MPC with perfect forecast, when regarding CSO but only slightly better for the WWTP volume. For the CC-MPC, both the total CSO and WWTP results are relatively close to the MPC with perfect forecast, but with the drawback of the distribution of the CSOs being significantly worse for the creek. Fig. 4 gives detailed volume comparisons for the controllable tanks under CC-MPC with different scaled bias through a two-day simulation (day 10 and day 11). The dynamics of Fig. 4 confirm that CC-MPC with an underestimated inflow performs significantly worse than that the CC-MPC with overestimated inflows. The explanation for this conclusion is also due to less conservative generated by the underestimated inflows. Moreover, the larger scales tend to have more differences in terms of tank volumes.

4.4. CC-MPC with various with offset biases

In this section, the bias is changed from a scaling to an offset, see (54). Both the CC-MPC and the MPC are tested with zero offset and three positive offsets. The sizes of the offsets are the annual mean inflow (0.02) times the factors of 1 and 0.25, and 10 times the dry-weather inflow (0.1)

$$E\{q\} = q^{actual} + b \tag{54}$$

The results of both MPC types can be seen in Tables 9 and 10 for the CSO and WWTP volume, respectively. We can observe that for both non-zero offsets, the CSO is significantly worse, with the offset of 0.1 being even worse. The results of the WWTP volume are also worse than the MPC with perfect forecast. Fig. 5 gives more information about the performance of CC-MPC under different offsets. The differences in tank volume among CC-MPC using different offsets are compared. As always, the more volume in the tank indicates an increased chance of having more CSOs. From Fig. 5, we can conclude that CC-MPC with 0.1 offset have more tank volume than that the offsets, which means, CC-MPC with 0.1 offset behaves worse than that of MPC. However, the CC-MPC with 0.005 and 0.02 did not show a clear trend.

From the above results, we can infer that the CC-MPC is capable of handling different type of uncertainties, and for those type of uncertainties, it performs similarly to the deterministic MPC. We can further see that the CC-MPC, while not performing that well with constant offset biases, these biases were also outside the uncertainty bound, practically making the CC-MPC as blind as the deterministic MPC. In real-world scenarios, the uncertainty of the inflow is not exactly as the one used here. Instead the uncertainty bound would vary across the prediction horizon, as would do the biases of the expected inflow.

5. Conclusion

A stochastic MPC has been applied to a hydrodynamic SWMM model of the Astlingen urban drainage benchmark network, using a chance-constraint formulation of MPC.

A comparison study of the application of both CC-MPC and MPC has been done for several scenarios and types of uncertainties in forecasts, involving both biases in the forecast to different sizes of the uncertainty. Based on the simulations, we can conclude that only the uncertainty regarding biases has an effect on the performance of CC-MPC. Furthermore, it could be observed that the performance of both type of MPC considered deteriorate similarly with respect to CSO volume, when the forecast overestimates the rain inflow. However, when the forecast underestimates the rain inflow, then the CC-MPC performs similarly to the ideal case, while the performances of deterministic MPC deteriorates.

Table 7
Overflow results of the SWMM simulations with different controllers: MPC and CC-MPC under different scaled bias.

Tank & Pipes	MPC −20%	CC-MPC −20%	MPC −10%	CC-MPC −10%	MPC 0%	CC-MPC 0%	MPC 10%	CC-MPC 10%	MPC 20%	CC-MPC 20%
T1	96 776	90 004	95 187	91 355	93 251	92 927	94 419	94 728	96 383	96 615
T2	16 727	16 801	15 957	16 023	15 484	15 544	15 384	15 383	15 317	15 316
T3	33 182	33 298	33 842	33 857	34 017	34 313	34 239	34 065	33 928	34 304
T4	5 938	5 960	5 191	5 206	4 814	4 814	4 730	4 729	4 714	4 713
T5	15 147	15 147	15 147	15 147	15 147	15 147	15 147	15 147	15 147	15 147
T6	39 252	39 082	38 341	38 296	37 950	37 946	37 790	37 770	37 908	37 836
P7	4 015	4 015	4 016	4 015	4 016	4 015	4 015	4 016	4 015	4 015
P8	16 195	16 190	16 208	16 195	16 207	16 191	16 188	16 203	16 188	16 191
P9	4 029	4 029	4 030	4 029	4 030	4 029	4 028	4 029	4 028	4 029
P10	4 841	4 843	4 837	4 841	4 838	4 842	4 843	4 839	4 843	4 842
River	188 805	182 242	186 369	182 623	183 754	183 778	184 949	185 094	186 519	187 129
Creek	47 297	47 126	46 387	46 341	45 996	45 990	45 834	45 815	45 952	45 880
Total	236 102	229 368	232 756	228 964	229 750	229 768	230 782	230 909	23 2470	233 008
R. %	−2.7488	0.8228	−1.4231	0.6155		−0.0131	−0.6503	−0.7292	−1.5047	−1.8367
C. %	−2.8285	−2.4567	−0.8501	−0.7501		0.0130	0.3522	0.3935	0.0957	0.2522
Tot. %	−2.7647	0.1663	−1.3084	0.3421		−0.0078	−0.4492	−0.5045	−1.1839	−1.4181

Table 8
Treated wastewater results of the SWMM simulations with different controllers: MPC, and CC-MPC under different scaled bias.

	MPC −20%	CC-MPC −20%	MPC −10%	CC-MPC −10%	MPC 0%	CC-MPC 0%	MPC 10%	CC-MPC 10%	MPC 20%	CC-MPC 20%
WWTP Vol.	3 765 554	3 772 166	3 769 365	3 772 992	3 772 057	3 772 159	3 771 015	3 770 672	3 769 214	3 768 942
Imp. %	−0.1724	0.0029	−0.0714	0.0248		0.0027	−0.0276	−0.0367	−0.0754	−0.0826

Table 9
Overflow results of the SWMM simulations with different controllers: MPC and CC-MPC under different off-set biases.

Tank & Pipes	MPC	CC-MPC 0	MPC 0.005	CC-MPC 0.005	MPC 0.02	CC-MPC 0.02	MPC 0.1	CC-MPC 0.1
T1	93 251	92 927	93 655	93 856	96 472	96 590	131 407	130 211
T2	15 484	15 544	15 387	15 450	15 453	15 452	15 847	15 511
T3	34 017	34 313	33 975	34 322	34 086	34 485	36 811	36 548
T4	4 814	4 814	4 728	4 728	4 639	4 644	4 465	4 465
T5	15 147	15 147	15 147	15 147	15 147	15 147	15 147	15 147
T6	37 950	37 946	37 916	37 961	37 877	37 780	37 907	37 763
P7	4 016	4 015	4 015	4 015	4 015	4 016	4 016	4 016
P8	16 207	16 191	16 188	16 193	16 188	16 203	16 203	16 203
P9	4 030	4 029	4 028	4 029	4 028	4 029	4 029	4 029
P10	4 838	4 842	4 843	4 842	4 843	4 839	4 839	4 839
River	183 754	183 778	183 922	184 536	186 828	187 360	224 718	222 925
Creek	45 996	45 990	45 959	46 005	45 920	45 825	45 952	45 808
Total	229 750	229 768	229 881	230 541	232 748	233 185	270 670	268 733
R. %		−0.0131	−0.0914	−0.4256	−1.6729	−1.9624	−22.2928	−21.3171
C. %		0.0130	0.0804	−0.0196	0.1652	0.3718	0.0957	0.4087
Tot. %		−0.0078	−0.0570	−0.3443	−1.3049	−1.4951	−17.8107	−16.9676

Table 10
Treated wastewater results of the SWMM simulations with different controllers: MPC, and CC-MPC under different off-set biases.

	MPC	CC-MPC 0	MPC 0.005	CC-MPC 0.005	MPC 0.02	CC-MPC 0.02	MPC 0.1	CC-MPC 0.1
WWTP Vol.	3 772 057	3 772 159	3 771 978	3 771 575	3 768 823	3 768 643	3 731 689	3 733 651
Imp. %		0.0027	−0.0021	0.0001	−0.0857	−0.0905	−1.0702	−1.0182

The analysis presented here can in the future, be extended from using historical resembling rain fall, to also include historical resembling uncertainty; with the uncertainty nature varying across the simulation. The future work on CC-MPC, can include easing the computation of the constraint distribution for nonlinear and/or non-normal distributed uncertainties.

Declaration of competing interest

The authors declare that they have no known competing financial interests or personal relationships that could have appeared to influence the work reported in this paper.

Appendix A. Linear transformation of truncated distributions

For our discussion of linear transformations of truncated distributions, consider the stochastic scalar variable X_T to be X truncated in the interval $[a, b]$, with X following some distribution F.

$$X_T \sim F_a^b(\theta_x) : a \leq X \leq b, \quad X \sim F(\theta_x)$$

For truncated distributions (Nadarajah & Kotz, 2006), the probability are given by

$$Pr\{X_T \leq x\} = \frac{Pr\{X \leq x\} - Pr\{X \leq a\}}{Pr\{X \leq b\} - Pr\{X \leq a\}}$$

Under the assumption that linear transformations are plausible for X, let us define $Y = cX + d$. For the linear transformation of X_T where $c > 0$, we consider the probability:

$$\begin{aligned} Pr\{cX_T + d \le z\} &= Pr\{X_T \le \frac{z-d}{c}\} \\ &= \frac{Pr\{X \le \frac{z-d}{c}\} - Pr\{X \le a\}}{Pr\{X \le b\} - Pr\{X \le a\}} \\ &= \frac{Pr\{Y \le z\} - Pr\{Y \le ca + d\}}{Pr\{Y \le cb + d\} - Pr\{Y \le ca + d\}} \end{aligned}$$

where it can be seen that the resulting probability corresponds to a truncated version of Y.

If we consider the case of $c < 0$:

$$\begin{aligned} Pr\{cX_T + d \le z\} &= 1 - Pr\{X_T \le \frac{z-d}{c}\} \\ &= 1 - \frac{Pr\{X \le \frac{z-d}{c}\} - Pr\{X \le a\}}{Pr\{X \le b\} - Pr\{X \le a\}} \\ &= \frac{Pr\{Y \le z\} - Pr\{Y \le cb + d\}}{Pr\{Y \le ca + d\} - Pr\{Y \le cb + d\}} \end{aligned}$$

where the truncated version of Y, has an inverted truncation interval.

From here, we can see that the linear transformation $Y_T = cX_T + d$ is itself a truncated distribution of the same distribution type as X_T, with the truncation interval also been linearly transformed:

$$Y_T \sim F_{a_y}^{b_y}(\theta_y) : a_y \le Y \le b_y, \quad Y \sim F(\theta_y)$$

$$a_y = \begin{cases} ca + d & c > 0 \\ cb + d & c < 0, \end{cases} \quad b_y = \begin{cases} cb + d & c > 0 \\ ca + d & c < 0 \end{cases}$$

Appendix B. Sum of truncated Gaussians

In a truncated distribution (Nadarajah & Kotz, 2006), the probability density function (PDF) is given by

$$f_{X_T}(x) = \frac{f_X(x)}{\Psi_X(a, b)} \tag{B.1}$$

$$\Psi_X(a, b) = Pr\{X \le b\} - Pr\{X \le a\} \tag{B.2}$$

where $f_X(x)$ is the PDF of the underlying distribution, and $\Psi_X(a, b)$ is the probability span of the truncation.

Let us now consider the sum of two independent truncated Gaussian distributions:

$$X_T \sim N_{a_x}^{b_x}(\mu_x, \sigma_x^2), \quad Y_T \sim N_{a_y}^{b_y}(\mu_y, \sigma_y^2) \tag{B.3}$$

It is clear that sum $X_T + Y_T$ is restricted to the interval $[a_z, b_z]$, as given below

$$a_z = a_x + a_y \le X_T + Y_T \le b_x + b_y = b_z \tag{B.4}$$

If we define the sum of the underlying distributions as $Z = X + Y$, then by using convolution (Hogg, McKean, & Craig, 2019) and the fact that X, Y is independent, we can rewrite the probability in terms of the underlying sum Z:

$$\begin{aligned} Pr\{X_T + Y_T \le z\} &= \int_{a_z}^{z} f_{X_T + Y_T}(\tau) d\tau \\ &= \int_{a_z}^{z} \int_{-\infty}^{\infty} f_{X_T, Y_T}(x, \tau - x) dx d\tau \\ &= \int_{a_z}^{z} \int_{-\infty}^{\infty} f_{X_T}(x) f_{Y_T}(\tau - x) dx d\tau \\ &= \int_{a_z}^{z} \frac{\int_{-\infty}^{\infty} f_X(x) f_Y(\tau - x) dx}{\Psi_X(a_x, b_x)\Psi_Y(a_y, b_y)} d\tau \\ &= \frac{\int_{a_z}^{z} f_{X+Y}(\tau) d\tau}{\Psi_X(a_x, b_x)\Psi_Y(a_y, b_y)} \end{aligned}$$

Given that the sum of Gaussian distributions is also Gaussian, we can conclude that the sum of truncated Gaussian distributions has an underlying Gaussian distribution, but is not defined as a scalar truncated distribution. We can write the probability of the sum in terms of probabilities:

$$Pr\{X_T + Y_T \le z\} = \frac{Pr\{Z \le z\} - Pr\{Z \le a_z\}}{\Psi_X(a_x, b_x)\Psi_Y(a_y, b_y)}$$

A scaled probability with similar shape to the probability of the scalar truncated distribution.

Appendix C. Assumption of conservative truncated sums

Given the interval in (B.4), the sum of $X_T + Y_T$ can in some sense be seen as a truncation of the underlying sum $Z = X + Y$. In CC-MPC, we want to consider the probability $Pr\{X_T + Y_T \le z\} \ge \gamma$, by considering the sum as a truncated Gaussian distribution Z_T, we can ease the computation, by assuming the following relation

$$Pr\{X_T + Y_T \le z\} \ge Pr\{Z_T \le z\} \ge \gamma \tag{C.1}$$

meaning Z_T is less likely to be below a certain value z than the true sum, and if it holds so does the probability of the true sum. Writing each probability out, the probability of each sum takes the forms

$$Pr\{Z \le z\} \ge Pr\{Z \le a_z\} + \gamma\Psi_X(a_x, b_x)\Psi_Y(a_y, b_y) \tag{C.2}$$

$$Pr\{Z \le z\} \ge Pr\{Z \le a_z\} + \gamma\Psi_Z(a_z, b_z) \tag{C.3}$$

The relation can be seen to hold if and only if the probability spans is related by

$$\Psi_Z(a_z, b_z) \ge \Psi_X(a_x, b_x)\Psi_Y(a_y, b_y) \tag{C.4}$$

The relation in (C.4), means that using the truncated sum provides a more conservative solution than using the true sum; given the right-hand side becomes larger.

In order to show the relation given in (C.4) is a fair assumption, let us rewrite the relation in terms of standard Gaussians, assuming the mean to be included in the intervals. The standard interval of a distribution i is then given by

$$\alpha_i = \frac{a_i - \mu_i}{\sigma_i}, \quad \beta_i = \frac{b_i - \mu_i}{\sigma_i} \tag{C.5}$$

and the relation by

$$\Psi(\alpha_z, \beta_z) \ge \Psi(\alpha_x, \beta_x)\Psi(\alpha_y, \beta_y) \tag{C.6}$$

Realizing that a probability span is bounded by $0 \le \Psi_i(a_i, b_i) \le 1$, then we have that the relation also holds if just one of the relations below holds

$$\Psi(\alpha_z, \beta_z) \ge \Psi(\alpha_x, \beta_x) \tag{C.7}$$

$$\Psi(\alpha_z, \beta_z) \ge \Psi(\alpha_y, \beta_y) \tag{C.8}$$

Given they are all given in the same distribution, this means that α_z, β_z has to fulfill

$$\alpha_z \le \alpha_x \quad \text{and} \quad \beta_z \ge \beta_x \tag{C.9}$$

or

$$\alpha_z \le \alpha_y \quad \text{and} \quad \beta_z \ge \beta_y \tag{C.10}$$

to ensure the relation.

From the definition in (C.5), we get that the interval of Z_T is given by

$$\alpha_z = \delta_x\alpha_x + \delta_y\alpha_y, \quad \delta_x = \frac{\sigma_x}{\sqrt{\sigma_x^2 + \sigma_y^2}} \tag{C.11}$$

$$\beta_z = \delta_x\beta_x + \delta_y\beta_y, \quad \delta_y = \frac{\sigma_y}{\sqrt{\sigma_x^2 + \sigma_y^2}} \tag{C.12}$$

By using contradiction we can now prove that β_z is larger than at least one of α_x, β_x. Consider

$$\beta_x \geq \delta_x \beta_x + \delta_y \beta_y \tag{C.13}$$

$$\beta_y \geq \delta_x \beta_x + \delta_y \beta_y \tag{C.14}$$

by isolating β_y, and combining the inequalities we get

$$(1-\delta_x)\beta_x \geq \frac{\delta_y \delta_x}{1-\beta_y}\beta_x \tag{C.15}$$

by rewriting in terms of the variances we get

$$0 \geq \sigma_x \sigma_y \tag{C.16}$$

which is infeasible, given variances are positive by default. Similarly, we can use the same approach, to prove that

$$\alpha_z \geq \alpha_x \quad \text{and} \quad \alpha_z \geq \alpha_y \tag{C.17}$$

cannot simultaneous be true.

In the case of symmetry $\alpha_i = -\beta_i$, these contradictions becomes sufficiently to determine the relation in (C.4) holds, given

$$\Psi(-\beta_z, \beta_z) \geq \Psi(-\beta_x, \beta_x)\Psi(-\beta_y, \beta_y) \tag{C.18}$$

The relation does not seem to have a simple prove, for the more general intervals. But based on the contradictions, then if X_T has the larger interval, $\beta_x \geq \beta_y$ and $\alpha_x \leq \alpha_y$, then Z_T has larger interval than Y_T, fulfilling the relation.

A final comment, given the uncertainties of each constraints in model in Section 2 is scaled by the same factors; only the size of the initial intervals in the uncertainties determines the size relations between the different α, β values. Furthermore, during the simulations in Section 4, the intervals where chosen such that in terms of the standard Gaussian, they were all $[-3/p, 3]$. Therefore, the intervals are identical and the relations holds.

Appendix D. Supplementary data

Supplementary material related to this article can be found online at https://doi.org/10.1016/j.conengprac.2021.104900.

References

Arellano-Garcia, H., & Wozny, G. (2009). Chance constrained water quality management model for reservoir systems: I. Strict monotonicity. *Computers & Chemical Engineering*, *33*(10), 1568–1583.

Cembrano, G., Quevedo, J., Salamero, M., Puig, V., Figueras, J., & Marti, J. (2004). Optimal control of urban drainage systems. Acase study. *Control Engineering Practice*, *12*, 1–9.

Cen, L., & Xi, Y. (2009). Aggregation-based model predictive control of urban combined sewer networks. In *Proc. of the 7th Asian control conference, Proc. of the 7th Asian control conference*.

Dhar, A., & Datta, B. (2006). Chance constrained water quality management model for reservoir systems. *ISH Journal of Hydraulic Engineering*, *12*(3), 39–48.

DWA German Association for Water,Wastewater and Waste (2005). *Guideline DWA-M 180E - Framework for planning of real time control of sewer networks*. DWA, accessed on 1 October 2019. URL https://webshop.dwa.de/de/guideline-dwa-m-180-december-2005.html.

Evans, M., Cannon, M., & Kouvaritakis, B. (2012). Linear stochastic MPC under finitely supported multiplicative uncertainty. In *Proc. of the 2012 American control conference*.

Garatti, S., Campi, M. C., Garatti, S., & Prandini, M. (2009). The scenario approach for systems and control design. *Annual Reviews in Control*, *33*, 149–157.

Gelormino, M. S., & Ricker, N. L. (1994). Model predictive control of a combined sewer system. *International Journal of Control*, *59*(3), 793–816.

Genceli, H., & Nikolaou, M. (1993). Robust stability analysis of constrained norm model predictive control. *AIChE Journal*, *39*, 1954–1965.

Grosso, J. M., Ocampo-Martinez, C., Puig, V., & Joseph-Duran, B. (2014). Chance-constrained model predictive control for drinking waternetworks. *Journal of Process Control*, *24*, 504–516.

Halvgaard, R., & Falk, A. K. V. (2017). Water system overflow modeling for model predictive control. In *Proceedings of the 12th IWA specialised conference on instrumentation, control and automation, Proceedings of the 12th IWA specialised conference on instrumentation, control and automation*.

Hogg, R. V., McKean, J. W., & Craig, A. T. (2019). *Introduction to mathematical statistics* (8th ed.). Boston: Pearson.

Horrace, W. C. (2005). Some results on the multivariate truncated normal distribution. *Journal of Multivariate Analysis*, *94*, 209–221.

Joseph-Duran, B., Meseguer, J., Cembrano, G., & Maruejouls, T. (2017). Closed-loop simulation of real-time controllers for urban drainage systems using high resolution hydraulic simulators. In *Proceedings of the 14th IWA/IAHR international conference on urban drainage*.

Karantonis, P., & Weber, C. (2016). Use of ISO measurement uncertainty guidelines to determine uncertainties in noise & vibration predictions and design risks. In *Proceedings of ACOUSTICS, Proceedings of ACOUSTICS*, Brisbane, Australia (pp. 1–9).

Kouvaritakis, B., & Cannon, M. (2016). *Advances textbooks in control and signal processing, Model predictive control - Classical, robust and stochastic*. Springer, http://dx.doi.org/10.1007/978-3-319-24853-0.

Lee, T., Wang, Q., & Tan, K. (1996). Robust smith-predictor controller for uncertain delay systems. *AIChE Journal*, *42*.

Maciejowski, J. M. (2002). *Predictive control: With constraints*. Pearson.

Magni, L., De Nicolao, G., Scattolini, R., & Allgöwer, F. (2003). Robust model predictive control for nonlinear discrete-time systems. *International Journal of Robust and Nonlinear Control*, *13*(3–4), 229–246.

Marinaki, M., & Papageorgiou, M. (2005). *Advances in industrial control, Optimal real-time control of sewer networks*. Springer.

Mesbah, A. (2016). Stochastic model predictive control: An overview and perspectives for future research. *IEEE Control Systems Magazine*, 30–44. http://dx.doi.org/10.1109/MCS.2016.2602087.

Müller, T., Schütze, M., & Bárdossy, A. (2007). Temporal asymmetry in precipitation time series and its influence on flow simulations in combined sewer systems. *Advances in Water Resources*, *107*, 56–64.

Nadarajah, S., & Kotz, S. (2006). R programs for computing truncated distributions. *Journal of Statistical Software*, *16*, code snippet 2.

Nicolao, G. D., Magni, L., & Scattolini, R. (1998). Stabilizing receding-horizon control of nonlinear time-varying systems. *IEEE Transactions on Automatic Control*, *43*, 1030–1036.

Ocampo-Martinez, C. (2010). *Advances in industrial control, Model predictive control of wastewater systems*. Springer.

Overloop, P. (2006). *Model Predictive Control on Open Water Systems*. Delft University Press: Delft.

Rossman, L. (2015). *Storm water management model users' manual version 5.1*. EPA - United States Environmental Protection Agency.

Schütze, M., Lange, M., Pabst, M., & Haas, U. (2018). Astlingen - a benchmark for real time control (RTC). *Water Science & Technology*, *2017*(2), 552–560.

Scott, P. (2003). Uncertainty in measurement: Noise and how to deal with it. In *Lab Manual*. URL http://physics.ucsc.edu/~drip/133/ch2.pdf.

Singh, V. P. (1988). *Hydrologic systems. Volume 1: Rainfall-runoff modelling*. Prentice Hall.

Sun, C., Cembrano, G., Puig, V., & Meseguer, J. (2018). Cyber-physical systems for real-time management in the urban water cycle. In *Proceedings of the 4th international workshop on cyber-physical systems for smart water networks* (pp. 3–5).

Sun, Z. Q., Dai, L., Liu, K., Xia, Y. Q., & Johansson, K. H. (2018). Robust MPC for tracking constrained unicycle robots with additive disturbances. *Automatica*, *90*, 172–184.

Sun, C., Joseph, B., Cembrano, G., Puig, V., & Meseguer, J. (2018). Advanced integrated real-time control of combined urban drainage systems using MPC: Badalona case study. In *13th international conference on hydroinformatic*, Palermo (pp. 2033–2041).

Sun, C., Joseph, B., Maruejouls, T., Cembrano, G., Muñoz, E., Meseguer, J., et al. (2017). Efficient integrated model predictive control of urban drainage systems using simplified conceptual quality models. In *14th IWA/IAHR international conference on urban drainage*, Prague (pp. 1848–1855).

Sun, C., Joseph-Duran, B., Maruejouls, T., Cembrano, G., Meseguer, J., Puig, V., et al. (2017). Real-time control-oriented quality modelling in combined urban drainage networks. In *Proceedings of the IFAC 2017 world congress* (pp. 4002–4007).

Sun, C., Puig, V., & Cembrano, G. (2020). Real-time control of urban water cycle under cyber-physical systems framework. *Water*, *12*(406).

Sun, C., Svensen, J. L., Borup, M., Puig, V., Cembrano, G., & Vezzaro, L. (2020). An MPC enabled SWMM implementation of the Astlingen RTC benchmaking network. *Water*, *12*(1034).

Svensen, J. L., Niemann, H. H., Falk, A. K. V., & Poulsen, N. K. (2021). Chance-constrained model predictive control - A reformulated approach suitable for sewer networks. *Advanced Control of Applications*, being reviewed for publication.

Svensen, J. L., Niemann, H. H., & Poulsen, N. K. (2019). Model predictive control of overflow in sewer networks: A comparison of two methods. In *Proc. of the 4th int. conf. on control and fault-toleran systems, Proc. of the 4th int. conf. on control and fault-toleran systems* (pp. 412–417).

Wan, Z., & Kothare, M. V. (2002). Robust output feedback model predictive control using off-line linear matrix inequalities. *Journal of Process Control*, *12*(7), 763–774.